HHS Public Access

Author manuscript

J Genet Genomics. Author manuscript; available in PMC 2021 March 20.

Published in final edited form as:

J Genet Genomics. 2020 March 20; 47(3): 157–165. doi:10.1016/j.jgg.2020.02.009.

Two homologous *INDOLE-3-ACETAMIDE (IAM) HYDRALASE* genes are required for the auxin effects of IAM in *Arabidopsis*

Yangbin Gao[1], **Xinhau Dai**[1], **Yuki Aoi**[2], **Yumiko Takebayashi**[3], **Liping Yang**[1,4], **Xiaorui Guo**[1,5], **Qiwei Zeng**[1,6], **Hanchuanzhi Yu**[1], **Hiroyuki Kasahara**[2,3], **Yunde Zhao**[1,*]

[1]Section of Cell and Developmental Biology, University of California San Diego, La Jolla, CA, 92093-0116, USA

[2]Institute of Global Innovation Research, Tokyo University of Agriculture and Technology, Tokyo, 183-0054, Japan.

[3]RIKEN Center for Sustainable Resource Science, Kanagawa, 230-0045, Japan.

[4]School of Life Sciences, Jilin Normal University, Siping, 136000, China.

[5]Key laboratory of Plant Ecology, Northeast Forestry University, Harbin, 150040, China.

[6]State Key Laboratory of Silkworm Genome Biology, Institute of Sericulture and Systems Biology, Southwest University, Chongqing, 400716, China.

Abstract

Indole-3-acetamide (IAM) was the first confirmed auxin biosynthetic intermediate in some plant pathogenic bacteria. Exogenously applied IAM or production of IAM by overexpressing the bacterial *iaaM* gene in *Arabidopsis* causes auxin overproduction phenotypes. However, it is still inconclusive whether plants use IAM as a key precursor for auxin biosynthesis. Herein, we report the isolation *IAM hydrolase* 1 (*IAMH1*) gene in *Arabidopsis* from a forward genetic screen for IAM-insensitive mutants that display normal auxin sensitivities. *IAMH1* has a close homolog named *IAMH2* that is located right next to *IAMH1* on chromosome IV in *Arabidopsis*. We generated *iamh1 iamh2* double mutants using our CRISPR/Cas9 gene editing technology. We show that disruption of the *IAMH* genes rendered *Arabidopsis* plants resistant to IAM treatments and also suppressed the *iaaM* overexpression phenotypes, suggesting that IAMH1 and IAMH2 are the main enzymes responsible for converting IAM into IAA in *Arabidopsis*. The *iamh* double mutants did not display obvious developmental defects, indicating that IAM does not play a major role in auxin biosynthesis under normal growth conditions. Our findings provide a solid foundation for clarifying the roles of IAM in auxin biosynthesis and plant development.

*Corresponding author. yundezhao@ucsd.edu (Y. Zhao).

Author Contributions

Y.G. and Y.Z. conceived and designed the research. X.D., Y.A., Y.T., L.Y., X.G., Q.Z., and H.Y. performed research. Y.G., H.K., and Y.Z. analyzed data. Y.G., H.K., and Y.Z. wrote the paper.

Keywords

Auxin; auxin biosynthesis; Indole-3-acetamide; *Arabidopsis*; CRISPR; IAMH1

1. Introduction

Auxin plays essential roles in many aspects of plant growth and development (Zhao, 2018, 2014). Auxin concentrations in plant cells need to be tightly controlled so that plants can grow properly in response to developmental and environmental signals. Plants have evolved a complex network to effectively modulate auxin concentrations. Auxin biosynthesis, degradation, and transport all contribute to establishing proper auxin concentrations in cells (Cheng et al., 2007; Davies et al., 1999; Galweiler et al., 1998; Leznicki and Bandurski, 1988; Staswick et al., 2005; Stepanova et al., 2008; Strader and Bartel, 2009; Tao et al., 2008; Zhao et al., 2013; Zheng et al., 2016). Recent studies have shown that spatially and temporally regulated auxin biosynthesis is involved in determining almost all of the major developmental processes including embryogenesis, seedling growth, vascular pattern formation, and flower development (Chen et al., 2016; Chen et al., 2014; Cheng et al., 2006; Zheng et al., 2013). Understanding the molecular mechanisms of auxin biosynthesis provides the necessary tools for effectively modulating auxin levels in plants, thus allowing us to improve agriculturally important traits such as branching and root architecture.

Auxin is generally believed to be synthesized through both tryptophan (Trp)-dependent and Trp-independent pathways (Zhao, 2014). Very little is known about the Trp-independent pathway. But a recent report demonstrates that the cytosolic indole synthase (INS) is a key enzyme in the elusive Trp-independent pathway and that mutants defective in INS functions display phenotypes during early embryogenesis (Wang et al., 2015). But the roles of INS in auxin biosynthesis remain controversial (Nonhebel, 2015). Trp-dependent pathways have also not been fully elucidated. It has been proposed that Trp may be converted to IAA, the main natural auxin in plants, through several routes (Zhao, 2014). Trp can be metabolized into tryptamine (TAM) and indole-3-pyruvate (IPA) by PLP-dependent decarboxylases and aminotransferases, respectively. It is also known that Trp can be converted into indole-3-acetaldoxime (IAOx) by CYP79B2 and CYP79B3 P450 monooxygenases (Zhao et al., 2002). Moreover, plants also produce indole-3-acetamide (IAM) and indole-3-acetonitrile (IAN) from Trp (Sugawara et al., 2009). All of the aforementioned Trp metabolites including TAM, IPA, IAOx, and IAM have been proposed as intermediates for auxin biosynthesis in plants. However, so far only IPA has been firmly established as an important auxin biosynthetic intermediate in plants (Mashiguchi et al., 2011; Stepanova et al., 2011; Won et al., 2011). Disruption of either IPA biosynthesis or metabolism in *Arabidopsis*, maize, and rice leads to dramatic developmental defects (Cheng et al., 2006; Gallavotti et al., 2008; Phillips et al., 2011; Yamamoto et al., 2007; Zhang et al., 2018). It has been shown that Trp is converted into IAA using IPA as the intermediate in two steps in the so-called TAA/YUC pathway (Dai et al., 2013). Trp is first metabolized into IPA by the TAA family of aminotransferases and subsequently the YUC family of monooxygenases catalyzes the conversion of IPA into IAA (Zhao, 2012). The TAA/YUC pathway is evolutionary conserved among plant species and it is required for all of the major developmental

processes in *Arabidopsis*. Therefore, the TAA/YUC pathway has been recognized as a major auxin biosynthesis pathway.

The roles of the other Trp metabolites in auxin biosynthesis and plant development have not been fully resolved. IAOx has long been recognized as a potential auxin biosynthesis precursor. Over accumulation of IAOx in *Arabidopsis* by either overexpressing the biosynthetic enzyme CYP79B2 or by inactivating IAOx metabolizing enzymes such as SUR1 and SUR2 leads to auxin overproduction (Boerjan et al., 1995; Delarue et al., 1998; Zhao et al., 2002). Although IAOx can be metabolized into IAA in *Arabidopsis*, the exact mechanisms by which IAOx is converted into IAA are not understood at present. It is generally accepted that IAOx probably is not a major intermediate for auxin biosynthesis for two reasons. First, complete elimination of IAOx production in *Arabidopsis* by knocking out both CYP79B2 and B3 does not lead to dramatic developmental defects. Second, IAOx is only produced in a limited number of plant species that produce indolic glucosinolates (Kasahara, 2016).

The biosynthetic route for IAOx is well understood, but the reactions from IAOx to IAA have not been elucidated. In contrast, enzymes responsible for converting some Trp metabolites such as IAN into IAA are known (Bartel and Fink, 1994), but the biosynthetic route for IAN and IAM are not well understood. IAN can be converted into IAA in plants when added to plant growth media. It was shown more than two-decade ago that IAN is converted into IAA by a family of nitrilases (Bartel and Fink, 1994). Mutations in nitrilase 1 (*nit1*) in *Arabidopsis* render the mutant resistant to exogenous IAN (Bartel and Fink, 1994). Under normal growth conditions, *nit1* mutants do not display obvious developmental defects probably because of the compensatory effects provided by NIT1 homologs in *Arabidopsis*. It is still an outstanding question whether nitrilases and IAN play an important role in auxin biosynthesis and plant development.

IAM was the first definitively identified intermediate used in Trp-dependent auxin biosynthesis pathways in bacteria. Plant pathogens such as agrobacterium and pseudomonas synthesize auxin from Trp when they infect plants (Comai and Kosuge, 1982; Yamada et al., 1985). The bacteria-produced auxin alters the growth and developmental patterns of the infected plant cells so that the pathogens can use the plant cells to produce carbon- and nitrogen- rich compounds for their growth. The pathogens convert Trp into IAM using the bacterial iaaM Trp-2-monooxygenase and subsequently the pathogen-encoded hydrolase iaaH converts IAM to IAA (Comai and Kosuge, 1982; Yamada et al., 1985). *Arabidopsis* and other plants produce IAM in the absence of a bacterial infection, suggesting that plants may use IAM as an auxin biosynthetic intermediate as well (Sugawara et al., 2009). Furthermore, IAM was proposed as an intermediate in a route that converts IAOx into IAA (Sugawara et al., 2009). It is well known that *Arabidopsis* and other plants have the capacity to convert IAM into IAA. Overexpression of *iaaM* in *Arabidopsis*, petunia, and tobacco led to auxin overproduction phenotypes (Eklof et al., 2000; Mezzetti et al., 2004; Romano et al., 1995). It is hypothesized that plant hydrolases can convert IAM produced by the iaaM transgene to generate IAA. Bioinformatics analyses have identified a small family of IAM hydrolases named as amidases that share significant homology to the bacterial iaaH proteins (Pollmann et al., 2003). *Arabidopsis* amidase I has been shown to have the capacity to

hydrolyze IAM into IAA in vitro and in *Arabidopsis* (Pollmann et al., 2003). However, the amidase mutants do not display much reduced sensitivity to exogenous IAM (Pollmann et al., 2003), suggesting that plants probably also use other unidentified hydrolases to convert IAM to IAA. Identification of additional enzymes that are responsible for converting IAM to IAA will help us to unambiguously determine whether IAM is a key auxin biosynthetic intermediate in plants and whether IAM-derived auxin plays an important role in plant growth and development. Understanding of how IAM is converted into IAA in plants will also clarify whether IAM is an important intermediate in metabolizing IAOx into IAA.

In this study, we present the identification of two homologous genes that encode Indole-3-acetamide hydrolases (IAMHs) responsible for converting IAM to IAA in *Arabidopsis*. *Arabidopsis* plants that lacked the IAMH activities were resistant to exogenous IAM. Mutations in the *IAMH* genes suppressed the auxin overproduction phenotypes caused by overexpression of *iaaM*, the bacterial auxin biosynthetic gene. The *iamh* mutants did not display any obvious growth and developmental defects under normal laboratory conditions, suggesting that the IAM-derived auxin probably is not the main source of auxin required for *Arabidopsis* development under normal growth conditions. This work identified the main enzymes for hydrolyzing IAM to IAA in *Arabidopsis* and clarified the roles of IAM in auxin biosynthesis and plant development.

2. Results

2.1. IAM promotes plant growth and activates the auxin reporter DR5-GUS

IAM is the key intermediate used by some plant pathogenic bacteria to synthesize auxin (Fig. 1A) (Comai and Kosuge, 1982; Yamada et al., 1985). The two-step pathway catalyzed by the bacterial iaaM and iaaH effectively converts Trp into IAA (Fig. 1A). The *iaaM* gene has been widely used to genetically modulate auxin levels in plants (Cheng et al., 2006; Eklof et al., 2000; Romano et al., 1995). *Arabidopsis* seedlings grown on IAM-containing media in light had much elongated hypocotyls and developed epinastic cotyledons (Fig. 1B). IAM also slightly inhibited the elongation of primary roots (Fig. 1B). IAM-treated plants resembled closely to the well-characterized *Arabidopsis* auxin overproduction mutants such as *YUC* overexpression lines and *sur1* (Boerjan et al., 1995; Zhao et al., 2001), suggesting that IAM either activates an auxin signaling pathway directly or IAM is converted into IAA, the active natural auxin. Interestingly, seedlings grown on IAA-containing media did not display long hypocotyls and epinastic cotyledon (Fig. 1B). Rather IAA mainly inhibited primary root elongation and stimulated lateral root initiation and elongation (Fig. 1B).

We investigated whether IAM activated the expression of the auxin reporter DR5-GUS. As shown in Fig. 1C, seedlings grown on IAM-containing media had much elevated expression levels of DR5-GUS in the cotyledons and true leaves compared to seedlings grown on regular media. Activation of DR5-GUS expression in aerial part by IAM is consistent with the observation that IAM mainly stimulated hypocotyl elongation and changed the shape of cotyledons (Fig. 1B). In contrast, IAA activated DR5-GUS expression in the roots (Fig. 1C). Our results indicated that IAM and IAA caused different developmental phenotypes in *Arabidopsis* seedlings (Fig. 1B & C). The observed differences were probably caused by differences in uptake and transport of the two compounds. It is very clear that IAM

treatment could activate the auxin reporter and caused phenotypes related to elevated auxin levels.

2.2. A genetic screen for mutants resistant to IAM

Arabidopsis seedlings grown on 20 μM IAM phenocopied the *YUC* overexpression plants, which produce elevated levels of auxin (Cheng et al., 2006; Zhao et al., 2001). Because auxin overproduction mutants display phenotypes different from those caused by IAA treatments and because previous genetic screens for auxin resistant mutants were mainly conducted using exogenous IAA or synthetic auxin 2,4-D, we initially hypothesized that a genetic screen for mutants that can suppress *YUC* overexpression lines would uncover novel auxin genes. We hypothesized that such a genetic screen might be able to identify genes that are important for auxin biosynthesis, conjugation, degradation, transport or auxin signaling. Unfortunately, the *YUC* overexpression lines were not stable and the strong lines were completely sterile. Therefore, genetic screens for suppressors/enhancers of *YUC* overexpression lines were not productive. Because of the strong phenotypic similarities between IAM-treated plants and the *YUC* overexpression lines, we believed that genetic screens for IAM resistant mutants would mimic the screens for suppressors of *YUC* overexpression lines.

We mutagenized *Arabidopsis* seeds using EMS and conducted the genetic screen using 7- to 9-day old seedlings grown on 20 μM IAM under light. The putative mutants should have short hypocotyls and normal cotyledon shapes. We screened M2 seeds from 1000 individual M1 plants and identified more than 100 putative IAM-resistant mutants, which were subsequently transplanted to soil. Among the putative mutants, many were dwarf with dark-green leaves, which are very similar to the brassinolide (BR) biosynthesis and signaling mutants. Such obvious BR mutants were discarded. We conducted second round screens with M3 seeds and confirmed 24 IAM-resistant mutants. One of the mutants, #483, was almost insensitive to IAM. Light grown mutant #483 had a short hypocotyl and flat cotyledons (Fig. 2A) when grown on 20 μM IAM, but the mutant was very similar to WT when grown on MS media (Fig. S1A). Activation of DR5-GUS expression by IAM was also suppressed in the mutant #483 (Figs. 2B and S2B). We backcrossed the mutant to WT Col and out-crossed it to WT Ler. About 25% seedlings from either F2 populations displayed the IAM resistant phenotype, suggesting that the phenotype was caused by a recessive mutation of a single locus.

2.3. Cloning of the IAMH1 gene

We mapped the mutation in the #483 mutant to the bottom of chromosome IV and narrowed the mapping interval down to a 330 Kb region. Among the ORFs in the mapping interval, *At4g37550* and *At4g37560* encode putative Acetamidase/Formamidases, which potentially have the hydrolase activities that can break an amide bond. We hypothesized that a mutation in *At4g37550* or *At4g37560* probably would abolish the conversion of IAM into IAA in *Arabidopsis*, thus causing the IAM-insensitive phenotypes. We sequenced the genomic DNA of *At4g37550* and *At4g37560* from the mutant #483 and identified a G to A conversion in the first exon of *At4g37550* (Fig. 2). The mutation converted a Trp codon to a premature stop codon (Fig. 2C), suggesting that the mutant is likely a null allele.

To confirm that the identified mutation in the *At4g37550* gene caused the observed IAM insensitive phenotype, we obtained a T-DNA insertion mutant of *At4g37550* from the ABRC stock center. The T-DNA mutant was also resistant to IAM treatment, demonstrating that #483 mutant phenotypes were caused by the disruption of *At4g37550*. We renamed #483 mutant *iamh1–1* (*IAM hydrolase 1*) and *At4g37550* gene *IAMH1*. The T-DNA allele was named *iamh1–2*.

To further demonstrate that we had identified the causal mutation in *iamh1–1*, we transformed *iamh1–1* plants with a construct that harbored the *At4g37550* genomic fragment including its own promoter. As shown in Fig. 2D, the *IAMH1* genomic fragment fully restored the IAM sensitivity of the *iamh1–1* mutant. We also expressed an IAMH1-GFP fusion under the control of the *IAMH1* promoter in the *iamh1–1* background. The GFP fusion could also fully rescue the *iamh1–1* phenotypes. Interestingly, the complementation transgenic lines appeared to have longer hypocotyls than wild type plants grown under the same conditions (Fig. 2D). The differences were probably caused by a slight overexpression of the transgenes. Such an observation further supports the hypothesis that IAMH1 is involved in converting IAM to IAA in *Arabidopsis*.

IAMH1-like genes have been identified in all of the plant genomes including *Chlamydomonas reinhardtii* and *Physcomitrella patens*. A phylogenetic analysis of the IAMH1proteins across representative plant species was shown in Fig. S2. IAMH1 is highly conserved throughout the plant kingdom, as shown in the multiple sequence alignment of IAMH1 proteins from various plant species (Fig. S3). For example, the *Chlamydomonas reinhardtii* IAMH1 protein share 75% amino acid sequence identity with the *Arabidopsis* IAMH1.

2.4. IAMH1 is broadly expressed and is not localized in the nucleus.

We expressed the *GUS* reporter under the control of the *IAMH1* promoter in *Arabidopsis*. At seedling stage, the *GUS* expression was broadly distributed in cotyledons, true leaves, and root tips (Fig. 3). At reproductive stage, GUS expression was observed in young flowers, gynoecia, and in inflorescences (Fig. 3). Expression of IAMH1-GFP fusion driven by *IAMH1* promoter showed that IAMH1 was clearly not expressed in the nucleus (Fig. 3)

2.5. Arabidopsis genome contains two copies of IAMH genes

Neither *iamh1–1* nor *iamh1–2* showed obvious developmental defects under normal growth conditions, despite that both mutant alleles were resistant to IAM. Blastp analysis using IAMH1 protein as query identified At4g37560 as a close homolog of IAMH1 in the *Arabidopsis* genome (Fig. 4). We named At4g37560 IAMH2. IAMH2 and IAMH1 share 90% amino acid sequence identity. Because of the high sequence homology, we hypothesized that IAMH2 might also play an important role in converting IAM into IAA in *Arabidopsis*. Functional redundancy between *IAMH1* and *IAMH2* may explain our observation that *iamh1–1* and *iamh1–2* did not show obvious developmental defects.

We obtained a T-DNA insertion mutant from the ABRC stock center to test whether *iamh2* was also resistant to IAM. As shown in Fig. 4B, *iamh2–1* had short hypocotyls and normal cotyledons when grown on 20 μM IAM whereas wild type plants developed long hypocotyls

and epinastic cotyledons, demonstrating that disruption of *IAMH2* also led to IAM resistance. These data suggest that IAMH2 likely has overlapping functions with IAMH1.

2.6. Construction of iamh1 iamh2 double mutants

In order to assess the roles of the *IAMH* genes in auxin biosynthesis and *Arabidopsis* development, we need to inactivate both *IAMH* genes simultaneously. The two *IAMH* genes are located at Chromosome IV as tandem repeats (Fig. 4A). It is virtually impossible to generate *iamh1 iamh2* double mutants by crossing two single mutants together because of the extremely tight linkage between the two genes. We employed our recently developed ribozyme-based CRISPR technology (Gao et al., 2016; Gao et al., 2015; Gao and Zhao, 2014) to generate *iamh2* mutations in the *iamh1–1* background. We obtained two potential loss-of-function *iamh2* alleles (Fig 4C): *iamh2–2* and *iamh2–3*. The *iamh2–2* contained a single bp insertion after the nucleotide 330 from the ATG start codon, which generated an immediate stop codon (Fig. 4C). Therefore, *iamh2–2* is likely a null allele. The *iamh2–3* allele harbored a 20 bp deletion from nucleotide 322 to 342 (A in the ATG start codon counts as the first nucleotide). Such a large deletion in *iamh2–3* was also likely to completely abolish *IAMH2* function. The mutations were confirmed by DNA sequencing (Fig. S4).

We backcrossed both *iamh2* alleles to wild type Col plants to segregate out the CRISPR/Cas9. Both *iamh1–1 iamh2–2* and *iamh1–1 iamh2–3* double mutants were viable and fertile (Fig. S5). In fact, we did not observe any obvious developmental defects in the *iamh* double mutants under normal plant growth conditions. Our data suggest that auxin-derived from IAM probably is not required for *Arabidopsis* growth and development under laboratory growth conditions.

2.7. Suppression of the iaaM overexpression phenotypes by disrupting the IAMH genes

The bacterial auxin biosynthetic gene *iaaM* encodes a Trp monooxygenase, which converts Trp to IAM (Fig. 1). Overexpression *iaaM* alone is sufficient to cause auxin overproduction phenotypes (Cheng et al., 2006; Romano et al., 1995). The *iaaM* overexpression lines display long hypocotyls and epinastic cotyledons at seedling stage (Fig. 5A). The overexpression lines also produce more upright and narrower true leaves with longer petioles at young adult stages (Fig. 5B). When we introduced the same construct into *iamh1–1 iamh2–3*, the auxin overproduction phenotypes disappeared (Fig. 5A and B), suggesting that IAMH enzymes are needed to convert endogenously produced IAM into IAA. Both WT and the *iamh1–1 iamh2–3* double mutants grew normally without the *iaaM* gene (Fig. S5).

We analyzed auxin concentrations in IAM treated plants, which had obvious auxin overproduction phenotypes (Fig. 1). The IAA concentrations in *iamh1 iamh2* double mutants were very similar to those observed in WT plants (Fig. 5C). WT plants grown on IAM-containing media had much elevated IAA concentrations (Fig. 5C). However, only a slight increase of IAA in the *iamh1 iamh2* double mutants was observed (Fig. 5C).

One of the effective mechanisms for plants to maintain auxin homeostasis is to conjugate IAA to amino acids (Staswick et al., 2005). We observed a dramatic increase of IAA-Asp and IAA-Glu in the IAM treated WT plants (Fig. 5D and E). In contrast, IAM treatment in

iamh1 iamh2 double mutants did not induce a substantial increase in IAA-Asp and IAA-Glu conjugates (Fig. 5D and E), further supporting that IAM was not adequately hydrolyzed into IAA in the *iamh1 iamh2* double mutants.

3. Discussion

Although IAM was the first confirmed Trp metabolite that could serve as an auxin precursor (Comai and Kosuge, 1982), its role in auxin biosynthesis in plants has never been clarified. In this paper, we uncovered two *IAMH* genes that encode hydrolases that are capable of converting IAM into IAA in *Arabidopsis*. We showed that *Arabidopsis* plants lacked the two *IAMH* genes were resistant to IAM treatments. Disruption of the *IAMH* genes also suppressed the developmental abnormalities caused by overexpression of the *iaaM* gene, suggesting that the IAMHs are the main enzymes in converting IAM into IAA in *Arabidopsis*. Together with previous findings that *Arabidopsis* plants contained measurable amount IAM (Sugawara et al., 2009), we conclude that IAM is a viable candidate for auxin biosynthesis in plants.

The *iamh1 iamh2* double mutants did not display obvious developmental defects under our normal growth conditions, suggesting that auxin synthesized from the IAM pathway may not play critical roles in *Arabidopsis* development. However, we noticed that *iamh1 iamh2* double mutants were not entirely insensitive to IAM (Fig. 5). IAM treatments still slightly increased IAA concentrations in the double mutants (Fig. 5). We also observed that both IAA-Asp and IAA-Glu were increased in the double mutants (Fig. 5), although the amplitudes of the increases were much smaller compared to those of WT treated with IAM. Our results suggest that *Arabidopsis* plants have other hydrolases that are capable of converting IAM to IAA. An obvious candidate is the Amidase1, which has been studied extensively for almost two decades (Pollmann et al., 2003). It will be interesting to further knock out the amidase family of genes in the *iamh1 iamh2* double mutant background. Analysis of the higher order mutants in terms of IAM sensitivity and developmental phenotypes will provide a more definitive answer to the roles of IAM in auxin biosynthesis and plant development.

In summary, we have identified two IAM hydrolase genes that are responsible for converting IAM into IAA in *Arabidopsis*. We showed that the *IAMH* genes are required for the auxin overproduction phenotypes caused by IAM treatments or by overexpressing the bacterial *iaaM* gene. Our findings provide a foundation for determining the roles of IAM in auxin biosynthesis and in plant development. Moreover, our findings will also help resolve the molecular mechanisms by which IAOx is converted into IAA.

4. Materials and Methods

4.1. Plant materials and growth conditions

The *iamh1–2* and *iamh2–1* T-DNA mutants were obtained from the *Arabidopsis* stock center. Plants were grown under long-day conditions (16-h light and 8-h dark) at 22 °C. Seeds were surfaced sterilized by 70% ethanol and air-dried on filter papers in the hood before placed on plates containing Murashige and Skoog (MS) media (supplemented with

IAA or IAM when indicated). The plates with seeds were then incubated at 4 °C for 2 days before placed in the growth chamber. Seedlings were grown on the plates in the growth chamber until 7–9 days old, and then transferred to soil if needed.

4.2. Screen for Arabidopsis mutants resistant to IAM

Wild type Columbia *Arabidopsis* seeds were mutagenized using Ethyl methanesulfonate (EMS) treatments. Seeds from each mutagenized plant were harvested individually and grown on MS media containing 20 μM IAM. WT plants have obviously elongated hypocotyls. IAM- resistant seedlings with reduced hypocotyl length were selected and further characterized. The *iamh1–1* mutant was backcrossed 2 times to WT Col to remove background mutations.

4.3. Plant transformation

Arabidopsis plants with different genetic backgrounds were transformed using corresponding T-DNA constructs in Agrobacteria *GV3101* using the floral dipping method described previously (Clough and Bent, 1998).

4.4. Constructs and transgenic plants

The *IAMH1* promoter was amplified from *Arabidopsis* genomic DNA. The 2.8 Kb *IAMH1*promoter was cloned into pBI101.3 plasmid to drive the expression of the *GUS* reporter (Beta-glucuronidase). The *IAMH1pro:GUS* construct was transformed into WT Col plants and T1 plants were selected on MS plates containing 50 μg/mL kanamycin.

The $IAMH1_{pro}$*:IAMH1* construct was made using pART27 as the backbone with the entire 5.5 Kb *IAMH1* genomic fragment, which includes the 2.8 Kb promoter region upstream of the start codon, the 2.0 Kb region coding region, and the 657 bp region after the stop codon. The *iamh1–1* plants were transformed with the $IAMH1_{pro}$*:IAMH1* construct and T1 plants were selected on MS plates containing 20 μM IAM. Plants showing restored IAM sensitivity were selected as complemented lines.

$IAMH1_{pro}$*:IAMH1-EGFP* construct was made using pART27 as the plasmid backbone. We fused the 4.9 Kb *IAMH1*genomic fragment, which included the 2.8 Kb promoter region and the 2.0 Kb region from the start codon to just before the stop codon, with the EGFP gene.

CRISPR construct targeting the *IAMH2* gene was generated using our ribozyme- based guide RNA CRISPR system described previously (Gao et al., 2015; Gao and Zhao, 2014). The CRISPR target site chosen for *IAMH2* gene was GTCCTCTTCCAGGAGATGAATGG, which is in the second exon and the 314 to 336 bp region counting from the ATG start codon in the cDNA. The *iamh1–1* plants were transformed with our CRISPR constructs and T1 plants were selected on MS plates containing 16 μg/mL hygromycin.

4.5. Genotyping the iamh1–1 mutant

Plants with *iamh1–1* mutation were genotyped using primers 5’- GATGACGCC-AAGCGTGTAAGC −3’ and 5’- CTGGGAATTCAGAGGTAAGCAC −3’ to amplify the genomic DNA and then digested with N*co*I. PCR products from WT plants would be cut

into two fragments (0.6 Kb + 0.9 Kb) while the PCR products from the *iamh1–1* mutant would appear as a single band (1.5 Kb).

4.6. Beta-glucuronidase (GUS) staining

GUS staining of *IAMH1*$_{pro}$*:GUS* plants and *DR5-GUS* plants were performed according to the previously described protocol (Zhao et al., 2001).

4.7. Confocal imaging of root tips

Root tips of *IAMH1*$_{pro}$*:IAMH1-EGFP* plants were stained using Propidium Iodide and visualized using a confocal microscope. The cell contour appeared as red florescence signal and IAMH1-EGFP fusion proteins appeared as green florescence signal.

4.8. Analysis of auxin metabolites

Plant materials were first frozen in liquid nitrogen and stored at −80°C. We homogenized about 30 mg frozen plant tissues in 0.3 mL of extraction buffer using a Tissue Lyser (Qiagen) with the 3 mm zirconia beads for 3 min. The extraction buffer (80% acetonitrile/1% acetic acid aqueous solution) contained [phenyl-$^{13}C_6$] IAA, [$^{13}C_4$, ^{15}N]IAA-Asp and [$^{13}C_5$, ^{15}N]IAA-Glu, which served as internal standards. Extracts were centrifuged at 13,000 × *g* for 3 min at 4°C, and the supernatant was collected. We repeated the extraction twice, but did not add additional internal standards. We combined the extracts and added 2 mL of 1% acetic acid/H_2O. Then the total volume was reduced to <1 mL by evaporation using a Speed Vac from Thermo Fisher Scientific. We then loaded the concentrated extracts onto a 1 mL Oasis HLB column (Waters), and washed the column with 1 mL 1% acetic acid/H_2O. We eluted IAA, IAA-Asp, and IAA-Glu with 2 mL 80% acetonitrile/1% acetic acid. The elute was then reduced to <1 mL by evaporation using a Speed Vac. We loaded the fraction containing IAA, IAA-Asp, and IAA-Glu onto a 1mL Oasis WAX column. After washing with 1 mL 1% acetic acid/H2O and subsequent 2 mL 80% acetonitrile/H_2O, we eluted IAA with 2 mL 80% acetonitrile/1% acetic acid. IAA-Asp and IAA-Glu were eluted with 2 mL 80% acetonitrile/0.8% formic acid. We used a Speed Vac to dry each fraction through evaporation. We re-dissolved each fraction in 30 μL 1% acetic acid/H_2O, and injected it into an Agilent 6420 Triple Quad system (Agilent) with a ZORBAX Eclipse XDB-C18 column (1.8 mm, 2.1×50 mm). IAA separation by HPLC followed the following conditions: We used solvent A (0.05% acetic acid/H_2O) and solvent B (acetonitrile/0.05% acetic acid) to generate certain solvent gradients. We first ran 3% solvent B for 3 min and then a gradient from 3% to 15% of solvent B over 20 min at a flow rate of 0.2 mL min^{-1} with column temperature set at 40°C. The MS/MS analysis conditions for IAA and [phenyl-$^{13}C_6$]IAA (positive ion mode) were conducted as previously described (Sugawara et al., 2015).

Conditions for HPLC separation of IAA-Asp and IAA-Glu were the following: Solvent A (0.1% formic acid/H_2O) and Solvent B (acetonitrile/0.05% formic acid were used for running the column. We used a gradient of 3% to 8% of solvent B for 2 min, a gradient of 8% to 11% of solvent B for 7min, and a gradient of 11% to 15% of solvent B over 15 min at a flow rate of 0.2 mL min^{-1} at 30°C. The following conditions were used the MS/MS analysis of IAA-Asp and [$^{13}C_4$, ^{15}N]IAA-Asp: Capillary = 4,000 V, fragmentor voltage = 95

V, collision energy = 19 V, dwell time = 250 ms, and MS/MS transition (*m/z*) = 291/130 for unlabeled IAA-Asp and 296/130 for [$^{13}C_4$, ^{15}N]IAA-Asp. We used the following conditions for MS/MS analysis of IAA-Glu and [$^{13}C_5$, ^{15}N]IAA-Glu: capillary = 4,000 V, fragmentor voltage = 95 V, collision energy = 20 V, dwell time = 250 ms and MS/MS transition (*m/z*) = 305/130 for unlabeled IAA-Glu and 311/130 for [$^{13}C_5$, ^{15}N]IAA-Glu.

4.9. Statistical analysis.

The developmental differences among *iamh* mutants, transgenic lines, and wild type plants were obvious and qualitative, rendering statistical analysis unnecessary. For auxin and auxin metabolite analysis, we conducted Student's t-test to determine whether the differences between samples were statistically significant. The actual *t*-value and *p*-value were provided in the text and in the figure legends.

Supplementary Material

Refer to Web version on PubMed Central for supplementary material.

Acknowledgment

This research was supported by the NIH grant R01GM114660 to YZ.

References

Bartel B, Fink GR, 1994 Differential regulation of an auxin-producing nitrilase gene family in *Arabidopsis thaliana*. Proc Natl Acad Sci U S A 91, 6649–6653. [PubMed: 8022831]

Boerjan W, Cervera MT, Delarue M, Beeckman T, Dewitte W, Bellini C, Caboche M, Van Onckelen H, Van Montagu M, Inze D, 1995 Superroot, a recessive mutation in *Arabidopsis*, confers auxin overproduction. Plant Cell 7, 1405–1419. [PubMed: 8589625]

Chen L, Tong J, Xiao L, Ruan Y, Liu J, Zeng M, Huang H, Wang JW, Xu L, 2016 YUCCA-mediated auxin biogenesis is required for cell fate transition occurring during de novo root organogenesis in *Arabidopsis*. J Exp Bot 67, 4273–4284. [PubMed: 27255928]

Chen Q, Dai X, De-Paoli H, Cheng Y, Takebayashi Y, Kasahara H, Kamiya Y, Zhao Y, 2014 Auxin overproduction in shoots cannot rescue auxin deficiencies in *Arabidopsis* roots. Plant Cell Physiol 55, 1072–1079. [PubMed: 24562917]

Cheng Y, Dai X, Zhao Y, 2006 Auxin biosynthesis by the YUCCA flavin monooxygenases controls the formation of floral organs and vascular tissues in *Arabidopsis*. Genes Dev 20, 1790–1799. [PubMed: 16818609]

Cheng Y, Dai X, Zhao Y, 2007 Auxin synthesized by the YUCCA flavin monooxygenases is essential for embryogenesis and leaf formation in *Arabidopsis*. Plant Cell 19, 2430–2439. [PubMed: 17704214]

Clough SJ, Bent AF, 1998 Floral dip: a simplified method for Agrobacterium-mediated transformation of *Arabidopsis thaliana*. Plant J 16, 735–743. [PubMed: 10069079]

Comai L, Kosuge T, 1982 Cloning characterization of iaaM, a virulence determinant of Pseudomonas savastanoi. J Bacteriol 149, 40–46. [PubMed: 6274847]

Dai X, Mashiguchi K, Chen Q, Kasahara H, Kamiya Y, Ojha S, DuBois J, Ballou D, Zhao Y, 2013 The biochemical mechanism of auxin biosynthesis by an *Arabidopsis* YUCCA flavin-containing monooxygenase. J Biol Chem 288, 1448–1457. [PubMed: 23188833]

Davies RT, Goetz DH, Lasswell J, Anderson MN, Bartel B, 1999 IAR3 encodes an auxin conjugate hydrolase from *Arabidopsis*. Plant Cell 11, 365–376. [PubMed: 10072397]

Delarue M, Prinsen E, Onckelen HV, Caboche M, Bellini C, 1998 Sur2 mutations of *Arabidopsis thaliana* define a new locus involved in the control of auxin homeostasis. Plant J 14, 603–611. [PubMed: 9675903]

Eklof S, Astot C, Sitbon F, Moritz T, Olsson O, Sandberg G, 2000 Transgenic tobacco plants co-expressing Agrobacterium iaa and ipt genes have wild-type hormone levels but display both auxin- and cytokinin-overproducing phenotypes. Plant J 23, 279–284. [PubMed: 10929121]

Gallavotti A, Barazesh S, Malcomber S, Hall D, Jackson D, Schmidt RJ, McSteen P, 2008 sparse inflorescence1 encodes a monocot-specific YUCCA-like gene required for vegetative and reproductive development in maize. Proc Natl Acad Sci U S A 105, 15196–15201. [PubMed: 18799737]

Galweiler L, Guan C, Muller A, Wisman E, Mendgen K, Yephremov A, Palme K, 1998 Regulation of polar auxin transport by AtPIN1 in *Arabidopsis* vascular tissue. Science 282, 2226–2230. [PubMed: 9856939]

Gao X, Chen J, Dai X, Zhang D, Zhao Y, 2016 An Effective Strategy for Reliably Isolating Heritable and Cas9-Free *Arabidopsis* Mutants Generated by CRISPR/Cas9-Mediated Genome Editing. Plant Physiol 171, 1794–1800. [PubMed: 27208253]

Gao Y, Zhang Y, Zhang D, Dai X, Estelle M, Zhao Y, 2015 Auxin binding protein 1 (ABP1) is not required for either auxin signaling or Arabidopsis development. Proc Natl Acad Sci U S A 112, 2275–2280. [PubMed: 25646447]

Gao Y, Zhao Y, 2014 Self-processing of ribozyme-flanked RNAs into guide RNAs in vitro and in vivo for CRISPR-mediated genome editing. J Integr Plant Biol 56, 343–349. [PubMed: 24373158]

Kasahara H, 2016 Current aspects of auxin biosynthesis in plants. Biosci Biotechnol Biochem 80, 34–42. [PubMed: 26364770]

Leznicki AJ, Bandurski RS, 1988 Enzymic synthesis of indole-3-acetyl-1-O-beta-d-glucose. II. Metabolic characteristics of the enzyme. Plant Physiol 88, 1481–1485. [PubMed: 11537439]

Mashiguchi K, Tanaka K, Sakai T, Sugawara S, Kawaide H, Natsume M, Hanada A, Yaeno T, Shirasu K, Yao H, McSteen P, Zhao Y, Hayashi K, Kamiya Y, Kasahara H, 2011 The main auxin biosynthesis pathway in *Arabidopsis*. Proc Natl Acad Sci U S A 108, 18512–18517. [PubMed: 22025724]

Mezzetti B, Landi L, Pandolfini T, Spena A, 2004 The defH9-iaaM auxin-synthesizing gene increases plant fecundity and fruit production in strawberry and raspberry. BMC Biotechnol 4, 4. [PubMed: 15113427]

Nonhebel HM, 2015 Tryptophan-Independent Indole-3-Acetic Acid Synthesis: Critical Evaluation of the Evidence. Plant Physiol 169, 1001–1005. [PubMed: 26251310]

Phillips KA, Skirpan AL, Liu X, Christensen A, Slewinski TL, Hudson C, Barazesh S, Cohen JD, Malcomber S, McSteen P, 2011 vanishing tassel2 encodes a grass-specific tryptophan aminotransferase required for vegetative and reproductive development in maize. Plant Cell 23, 550–566. [PubMed: 21335375]

Pollmann S, Neu D, Weiler EW, 2003 Molecular cloning and characterization of an amidase from *Arabidopsis thaliana* capable of converting indole-3-acetamide into the plant growth hormone, indole-3-acetic acid. Phytochemistry 62, 293–300. [PubMed: 12620340]

Romano CP, Robson PR, Smith H, Estelle M, Klee H, 1995 Transgene-mediated auxin overproduction in *Arabidopsis*: hypocotyl elongation phenotype and interactions with the hy6–1 hypocotyl elongation and axr1 auxin-resistant mutants. Plant Mol Biol 27, 1071–1083. [PubMed: 7766890]

Staswick PE, Serban B, Rowe M, Tiryaki I, Maldonado MT, Maldonado MC, Suza W, 2005 Characterization of an *Arabidopsis* enzyme family that conjugates amino acids to indole-3-acetic acid. Plant Cell 17, 616–627. [PubMed: 15659623]

Stepanova AN, Robertson-Hoyt J, Yun J, Benavente LM, Xie DY, Dolezal K, Schlereth A, Jurgens G, Alonso JM, 2008 TAA1-mediated auxin biosynthesis is essential for hormone crosstalk and plant development. Cell 133, 177–191. [PubMed: 18394997]

Stepanova AN, Yun J, Robles LM, Novak O, He W, Guo H, Ljung K, Alonso JM, 2011 The *Arabidopsis* YUCCA1 flavin monooxygenase functions in the indole-3-pyruvic acid branch of auxin biosynthesis. Plant Cell 23, 3961–3973. [PubMed: 22108406]

Strader LC, Bartel B, 2009 The *Arabidopsis* PLEIOTROPIC DRUG RESISTANCE8/ABCG36 ATP binding cassette transporter modulates sensitivity to the auxin precursor indole-3-butyric acid. Plant Cell 21, 1992–2007. [PubMed: 19648296]

Sugawara S, Hishiyama S, Jikumaru Y, Hanada A, Nishimura T, Koshiba T, Zhao Y, Kamiya Y, Kasahara H, 2009 Biochemical analyses of indole-3-acetaldoxime-dependent auxin biosynthesis in *Arabidopsis*. Proc Natl Acad Sci U S A 106, 5430–5435. [PubMed: 19279202]

Tao Y, Ferrer JL, Ljung K, Pojer F, Hong F, Long JA, Li L, Moreno JE, Bowman ME, Ivans LJ, Cheng Y, Lim J, Zhao Y, Ballare CL, Sandberg G, Noel JP, Chory J, 2008 Rapid synthesis of auxin via a new tryptophan-dependent pathway is required for shade avoidance in plants. Cell 133, 164–176. [PubMed: 18394996]

Wang B, Chu J, Yu T, Xu Q, Sun X, Yuan J, Xiong G, Wang G, Wang Y, Li J, 2015 Tryptophan-independent auxin biosynthesis contributes to early embryogenesis in *Arabidopsis*. Proc Natl Acad Sci U S A 112, 4821–4826. [PubMed: 25831515]

Won C, Shen X, Mashiguchi K, Zheng Z, Dai X, Cheng Y, Kasahara H, Kamiya Y, Chory J, Zhao Y, 2011 Conversion of tryptophan to indole-3-acetic acid by TRYPTOPHAN AMINOTRANSFERASES OF *ARABIDOPSIS* and YUCCAs in *Arabidopsis*. Proc Natl Acad Sci U S A 108, 18518–18523. [PubMed: 22025721]

Yamada T, Palm CJ, Brooks B, Kosuge T, 1985 Nucleotide sequences of the Pseudomonas savastanoi indoleacetic acid genes show homology with Agrobacterium tumefaciens T-DNA. Proc Natl Acad Sci U S A 82, 6522–6526. [PubMed: 16593610]

Yamamoto Y, Kamiya N, Morinaka Y, Matsuoka M, Sazuka T, 2007 Auxin biosynthesis by the YUCCA genes in rice. Plant Physiol 143, 1362–1371. [PubMed: 17220367]

Zhang T, Li R, Xing J, Yan L, Wang R, Zhao Y, 2018 The YUCCA-Auxin-WOX11 Module Controls Crown Root Development in Rice. Front Plant Sci 9, 523. [PubMed: 29740464]

Zhao Y, 2012 Auxin biosynthesis: a simple two-step pathway converts tryptophan to indole-3-acetic acid in plants. Mol Plant 5, 334–338. [PubMed: 22155950]

Zhao Y, 2014 Auxin biosynthesis. *Arabidopsis* Book 12, e0173. [PubMed: 24955076]

Zhao Y, 2018 Essential Roles of Local Auxin Biosynthesis in Plant Development and in Adaptation to Environmental Changes. Annu Rev Plant Biol 69, 417–435. [PubMed: 29489397]

Zhao Y, Christensen SK, Fankhauser C, Cashman JR, Cohen JD, Weigel D, Chory J, 2001 A role for flavin monooxygenase-like enzymes in auxin biosynthesis. Science 291, 306–309. [PubMed: 11209081]

Zhao Y, Hull AK, Gupta NR, Goss KA, Alonso J, Ecker JR, Normanly J, Chory J, Celenza JL, 2002 Trp-dependent auxin biosynthesis in *Arabidopsis*: involvement of cytochrome P450s CYP79B2 and CYP79B3. Genes Dev 16, 3100–3112. [PubMed: 12464638]

Zhao Z, Zhang Y, Liu X, Zhang X, Liu S, Yu X, Ren Y, Zheng X, Zhou K, Jiang L, Guo X, Gai Y, Wu C, Zhai H, Wang H, Wan J, 2013 A role for a dioxygenase in auxin metabolism and reproductive development in rice. Dev Cell 27, 113–122. [PubMed: 24094741]

Zheng Z, Guo Y, Novak O, Chen W, Ljung K, Noel JP, Chory J, 2016 Local auxin metabolism regulates environment-induced hypocotyl elongation. Nat Plants 2, 16025. [PubMed: 27249562]

Zheng Z, Guo Y, Novak O, Dai X, Zhao Y, Ljung K, Noel JP, Chory J, 2013 Coordination of auxin and ethylene biosynthesis by the aminotransferase VAS1. Nat Chem Biol 9, 244–246. [PubMed: 23377040]

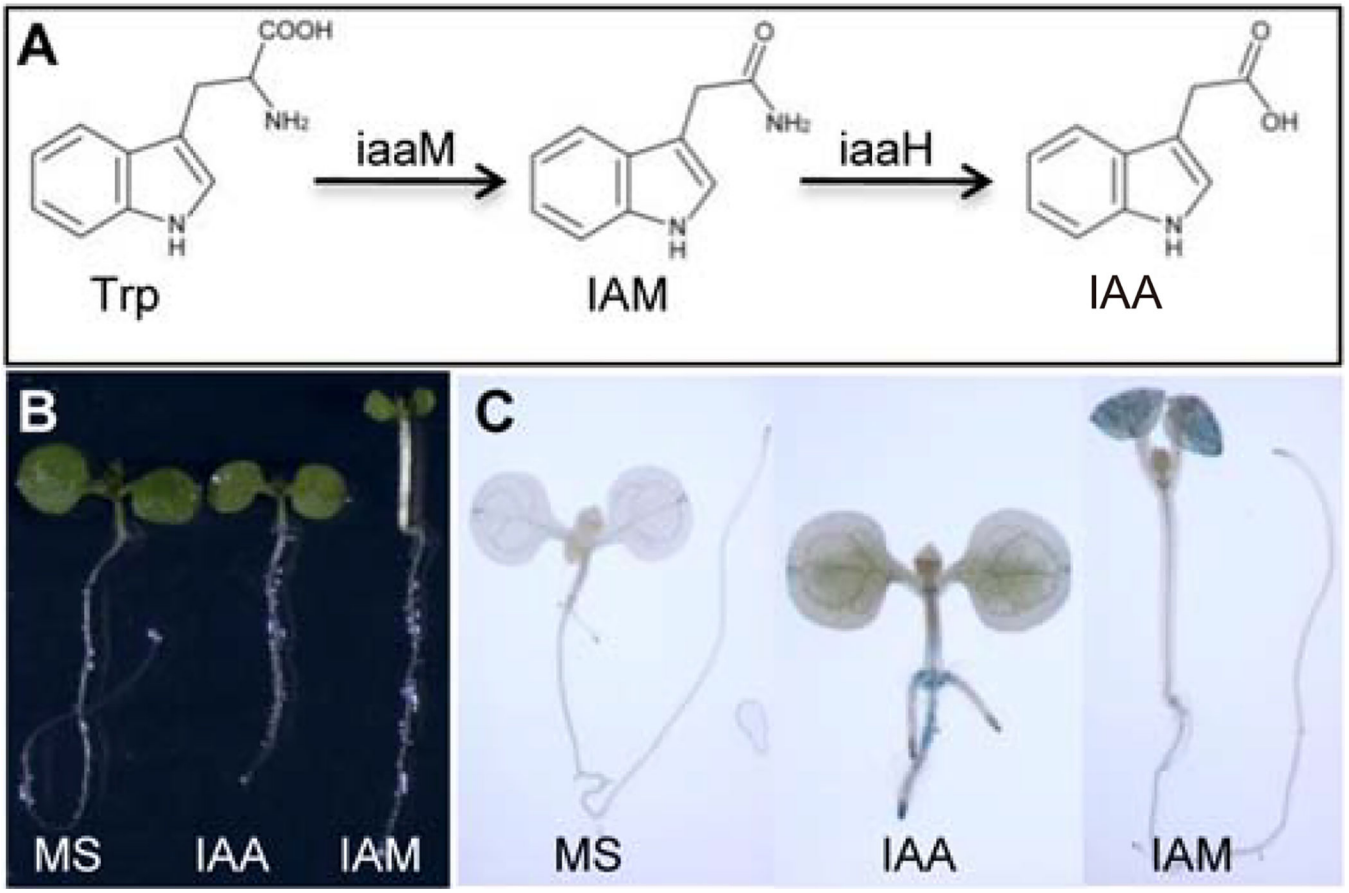

Fig 1.

Indole-3-acetamide (IAM) is a potential auxin biosynthetic intermediate in plants and IAM treatments affect plant growth and activate the auxin reporter DR5-GUS. **A**: A proposed Trp-dependent auxin biosynthetic pathway using IAM as the intermediate. This pathway is used by plant pathogenic bacteria such as Agrobacteria, which uses the iaaM and iaaH genes to convert Trp to IAA. The roles of IAM in plant auxin biosynthesis are not clear. **B**: Five-day old *Arabidopsis* seedlings grown on MS media and media containing 20 μM IAA or IAM. Note that IAA inhibits primary root elongation and IAM stimulates hypocotyl growth. Note that the seedling above the label IAA and IAM refer to seedlings grown on IAA and IAM-containing media, respectively. **C**: Activation of DR5-GUS expression by IAA and IAM. Interestingly, IAM mainly activates DR5-GUS expression in aerial tissue whereas IAA increases DR5-GUS signal in the root.

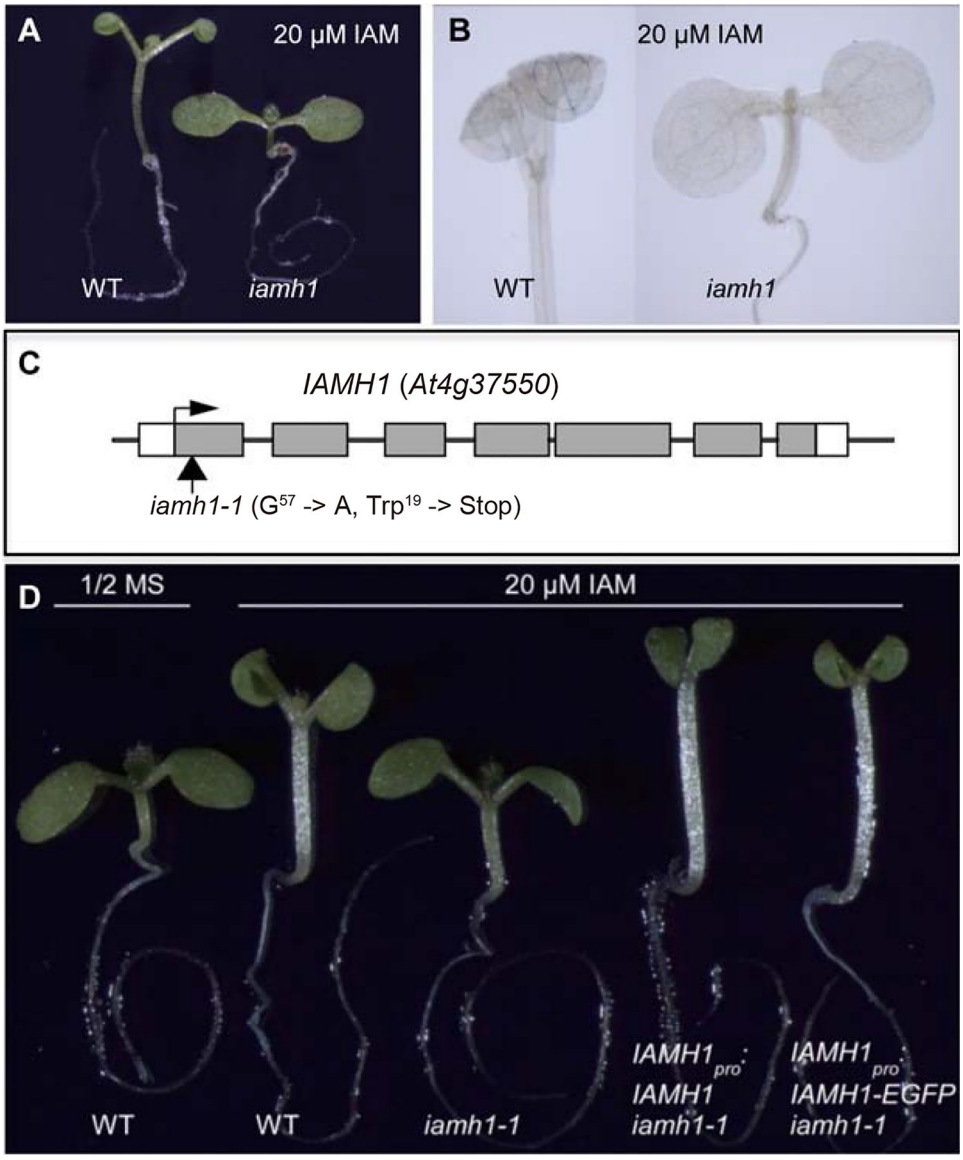

Fig 2.

Isolation and cloning of an IAM resistant mutant (*iamh1*). **A**: Isolation of an IAM-resistant mutant, which does not have elongated hypocotyl and does not display epinastic cotyledons when grown on 20 μM IAM-containing media. **B**: The expression of DR5-GUS auxin reporter is not induced by IAM treatments in the *iamh1* mutant. **C**: The *iamh1* mutation was identified by map-based positional cloning. The *IAMH1* gene is *At4g37550*. The *iamh1–1* mutant harbors a G to A mutation in *At4g37550* that results in a premature stop codon. **D**: The *iamh1* phenotypes are rescued by wild type *IAMH1* genomic DNA or *IAMH1* genomic DNA fused with GFP driven by the *IAMH1* promoter.

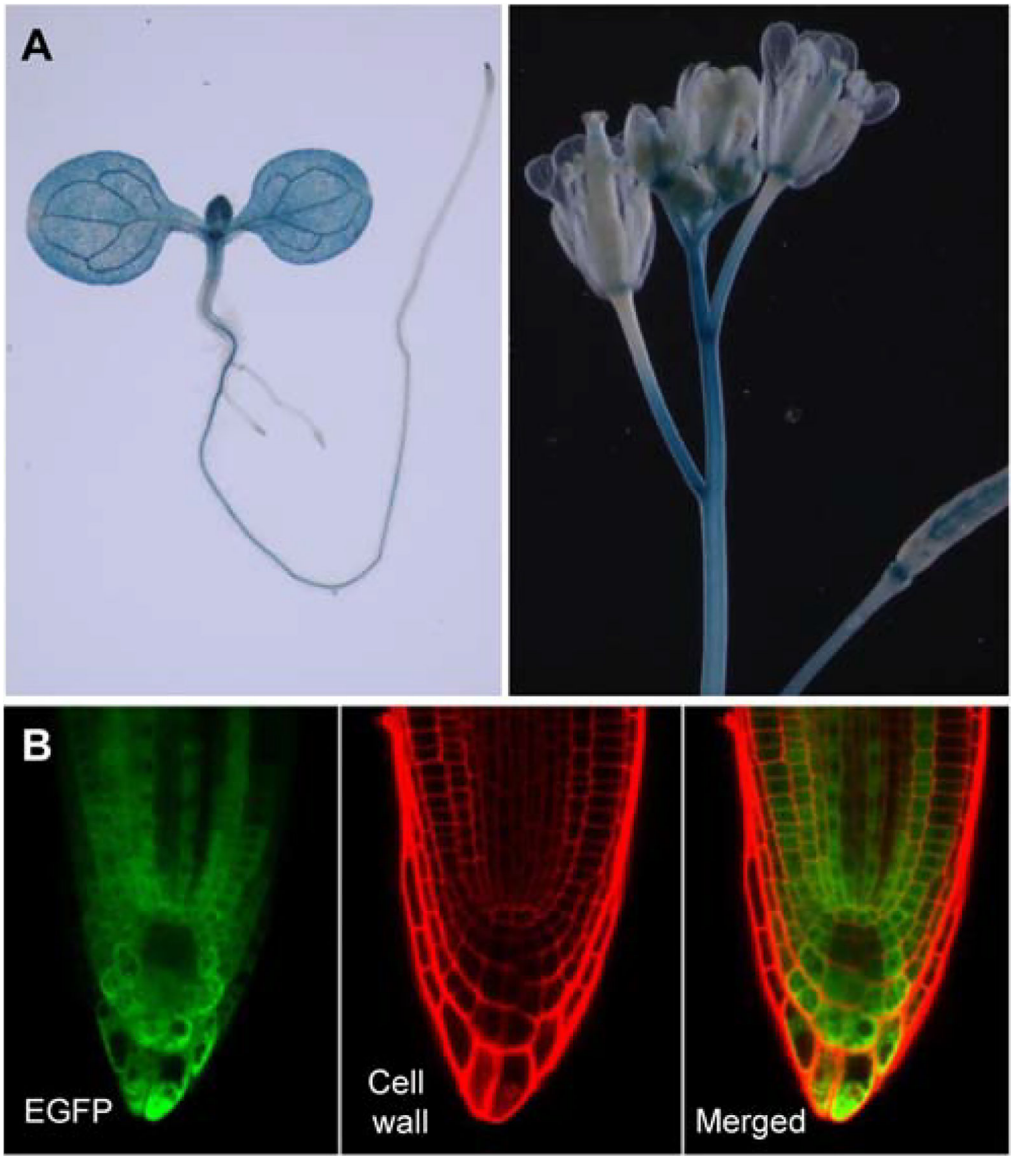

Fig 3.

Expression pattern of *iamH1* and sub-cellular localization of IAMH1 protein. **A**: The GUS expression patterns of $IAMH1_{pro}$*:GUS* Transgenic lines. Note that the reporter has a broad expression pattern. **B**: Expression of the IAMH1-EGFP fusion in *Arabidopsis* roots driven by the *IAMH1* promoter. IAMH1 appears to be located in the cytosol.

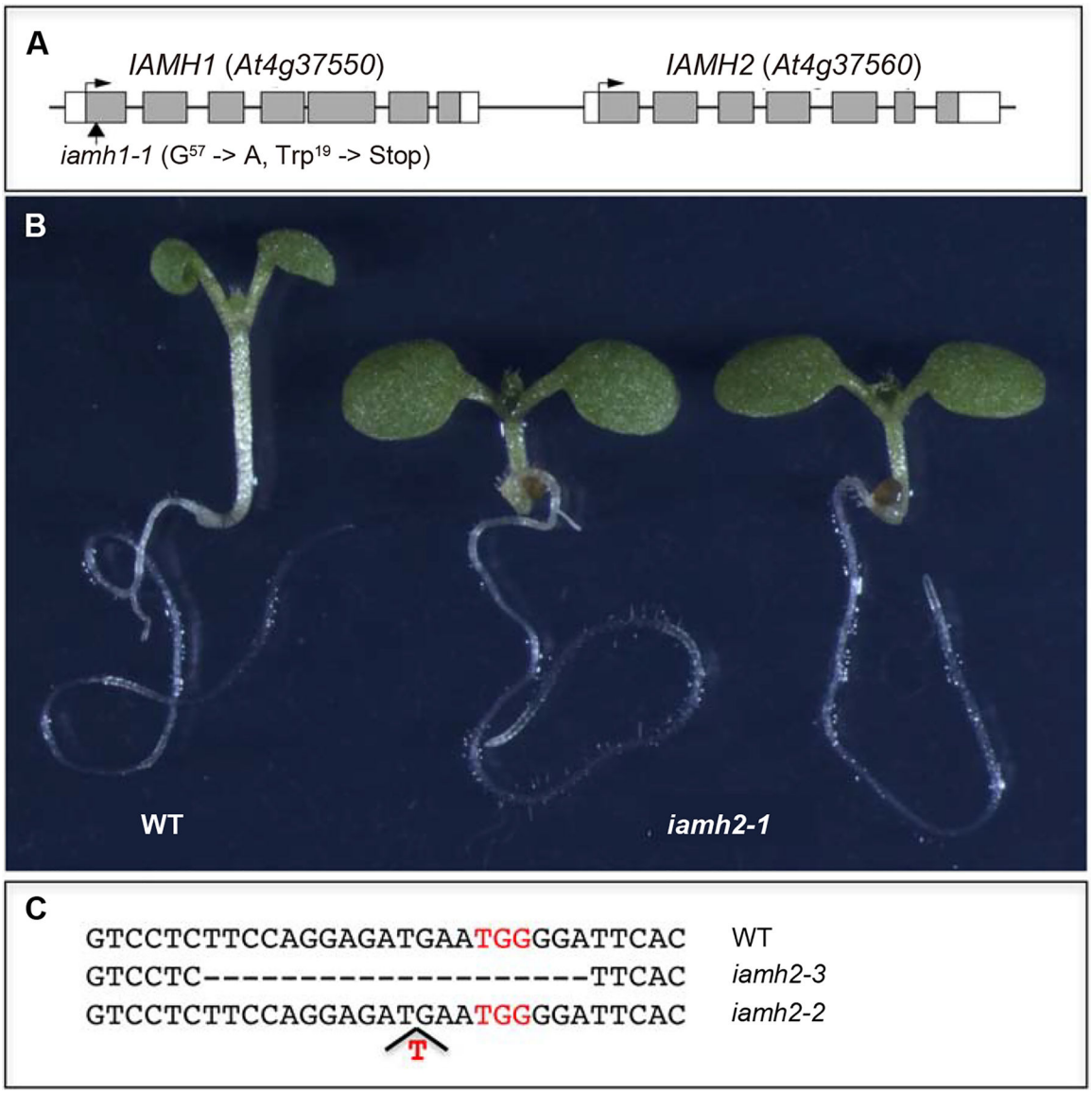

Fig 4.

The *IAMH2* gene is also involved in converting IAM into IAA. **A**: *IAMH1* has a close homolog, *IAMH2*. The two genes are tandem repeats located on Chromosome IV. **B**: A T-DNA insertion in *IAMH2* also caused resistance to exogenous IAM. **C**: Generation of *iamh2* alleles in *iamh1–1* by CRISPR/Cas9 gene editing technology. TGG in red is the PAM site for CRISPR/Cas9. The *iamh2–2* allele harbors one T insertion and *iamh2–3* contains a 20 bp deletion.

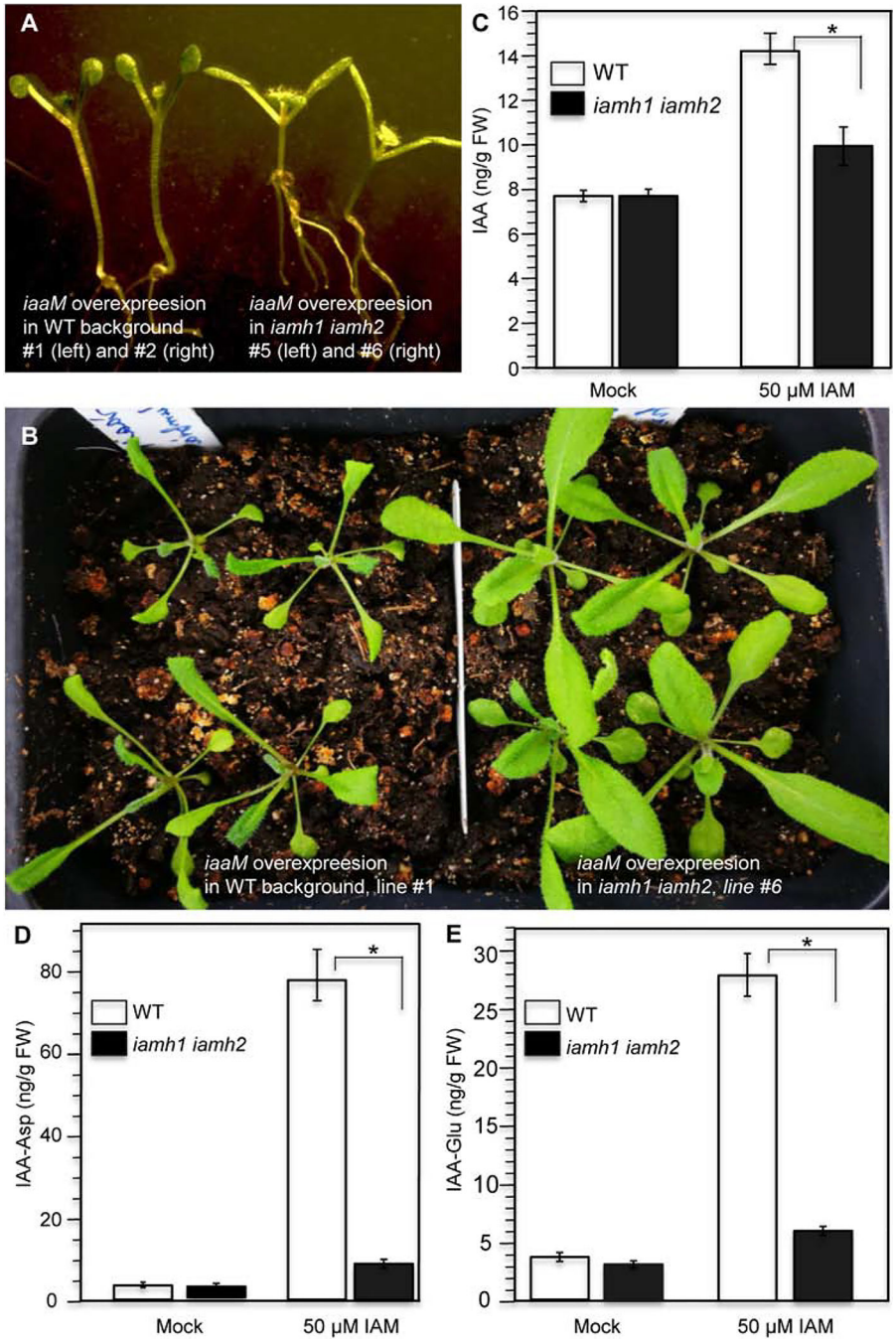

Fig 5.

The *IAMH* genes are major contributors to hydrolysis of IAM in *Arabidopsis*. **A**: Disruption of the *IAMH* genes suppressed the *iaaM* overexpression phenotypes. Note that overexpression of the bacterial *iaaM* gene led to long hypocotyls and epinastic cotyledons (left, two independent T1 plants), which are characteristic auxin overproduction phenotypes. **B**: Young adult independent T1 plants of *iaaM* overexpression lines in WT (left) and in the *iamh1 iamh2 −3* background (right). **C**: WT and the double mutants contained similar levels of IAA (*t*-value = −0.31235; *P*-value = 0.385191.). However, IAM treatment caused a

dramatic increase of IAA in WT plants, but much less increase in the *iamh1–1 iamh2–3* double mutants background (*t*-value = 6.55; *P*-value = 0.001404). **D**: IAM treatment caused about 80-fold increase of IAA-Asp conjugate in wild type, but only a slight increase in the *iamh1–1 iamh2–3* double mutants (*t*-value = 19.95751; *P*-value = 0.000019). **E**: IAM treatment led to an increase in IAA-Glu synthesis in WT, but the increase was very small in the *iamh1–1 iamh2–3* double mutants (*t*-value = 13.28318; *P*-value = 0.000093). * indicates statistically significant.